

Potentiometric Study on Interaction of Dodecyltrimethylammonium Bromide with α-Amylase

Abdol-Khalegh Bordbar,* Reza Hosseinzadeh, and Khodayar Omidiyan

Department of Chemistry, University of Isfahan, Isfahan, 81746-73441, Iran

Received January 6, 2004; E-mail: bordbar@sci.ui.ac.ir

The binding of dodecyltrimethylammonium bromide (DTAB) with α-amylase was investigated under various experimental conditions, such as pH, ionic strength, urea and protein concentration at 25 °C using surfactant membrane-selective electrodes as a fast and accurate method. The obtained binding isotherms have been analyzed and interpreted using the Wyman binding potential concept. The results represent: a) the self aggregation of protein that occurs at enzyme concentrations of more than 1 mg/mL (this observation was also confirmed by light-scattering measurements), b) the binding affinity at 10^{-3} M NaBr is more than other salt concentrations, and c) in the concentration range of 3 to 5 M of urea a predominant unfolding of protein occurs.

Amylases are enzymes that hydrolyse starch molecules to give diverse products, including dextrins and progressively smaller polymers composed of glucose units.[1,2] These enzymes are of great significance in present-day biotechnology with applications ranging from food, fermentation, textile to paper industries.[1,3]

Although amylases can be derived from several sources, including plants, animals, and microorganisms, microbial enzymes generally meet industrial demands. Today a large number of microbial amylases are commercially available and have almost completely replaced the chemical hydrolysis of starch in the starch processing industry.[3] The history of amylases began in 1811 when the first starch-degrading enzyme was discovered by Kirchhoff. This was followed by several reports of digestive amylases and malt amylases. It was much later, in 1930, that Ohlsson suggested a classification of starch digestive enzymes in malt as α- and β-amylases according to the anomeric type of sugars produced by the enzyme reaction. α-Amylase (1,4-α-D-glucan-glucanhydrolase, EC. 3.2.1.1) is a widely distributed secretary enzyme.[1] This enzyme hydrolyse internal (1 → 4)-α-glucosidic bonds in amylose, amylopectin, and related oligosaccharides. It is synthesized denovo in the aleurone layers in response to gibberellic acid. α-Amylases from various sources are characterized with respect to various parameters, such as the pH and temperature optima and stability, and the effects of activators, stabilizers, and inhibitors on their activity; these properties are exploited for their use in brewing and bread making industries.[4–7]

Enzyme contains two half-parts, the *N*-terminal one containing the active site and a *C*-terminal tail, a tandem repeated-unit structure possibly involved in raw starch binding.[8] Food emulsions and foams are generally stabilized by the adsorption of surface-active materials at the aqueous–oil and aqueous–air interfaces, respectively. These materials are often proteins or low-molecular-weight amphipathic emulsifiers (surfactants), or a combination of both of these species. Proteins and emulsifiers not only compete for adsorption sites at the interfaces, but interact in the bulk aqueous phase to form a range of protein–surfactant complexes that are themselves surface active.

Thus, it is important to understand the stabilization of food emulsions and foams by which the interactions between the proteins and surfactants that lead to the formation of such complexes are characterized. It is generally accepted that the binding of ionic surfactant molecules to proteins disrupts the native structure of most globular proteins.[9–11] This initially involves the ionic binding of surfactants to the ionic sites of the protein. Further binding occurs by hydrophobic cooperative interactions.[12,13] Hence, ionic surfactants interact with proteins through a combination of electrostatic and hydrophobic forces. In these systems, the thermodynamics of this interaction depends on the kind of surfactant and protein used.

In the present study, the binding of dodecyltrimethylammonium bromide (DTAB) to α-amylase was investigated under various experimental conditions using ion-selective membrane electrodes as a fast and accurate method. The binding data were analyzed based on a known binding model, and interpreted from a structural view point, which led to the formation of DTAB–α-amylase complexes, which were characterized. The results of such a study can be useful with respect to wild applications of α-amylase and surfactants in food industries.

Experimental

Materials. α-Amylase enzyme (Bacillus Subtilis) and dodecyltrimethylammonium bromide (DTAB) were obtained from Sigma Chemical Co. Dioctyl phthalate (DOP) obtained from Aldrich Chemical Co. Tetrahydrofuran (THF), acetone, nitric acid (65%), sodium hydroxide, sodium bromide, diphosphorus pentaoxide (P_2O_5), ethanol, carboxylated PVC, high molecular weight, sodium phosphate, and sodium hydrogenphosphate were obtained from Merck Chemical Co. Silver wire and a sodium reference electrode (serial num. 6.0501.100) were purchased from Metrohm Co. Urea of high purity was purchased from Isfahan scientific and industrial research center. All of the materials have a high degree of purity. All of the solutions were prepared by double-distilled water. The enzyme solutions were freshly prepared and used. The value of 69000 D was taken as the molecular weight of α-

Published on the web November 11, 2004; DOI 10.1246/bcsj.77.2027

amylase in all calculations.[14]

Apparatus. For all of the potentiometric measurements we used a potentiometer (Metrohm model, 744). Also, for determining the concentration of urea solutions, we used an Abbe refractometer. The light-scattering intensity was measured using a Shimadzu RF-5000 spectrofluoremeter with a thermostat cell compartment.

Emf Measurements. The surfactant membrane electrode selective to DTAB ion was constructed using a literature method.[15,16] The membrane contains specially conditioned PVC and DOP as a commercially available polymeric plasticizer. The PVC used in the present work contained negatively charged groups, which were neutralized by DTAB ion before use. The principle of this electrodes shows that the monomer DTAB activities in various solutions can be obtained from emf measurements on the following cell:

$$\mathrm{Ag/AgBr}\left|\begin{matrix}\text{internal}\\ \text{solution}\end{matrix}\right|\begin{matrix}\text{PVC}\\ \text{membrane}\end{matrix}\left|\begin{matrix}\text{testing solution}\\ \text{of DTAB}\end{matrix}\right|\begin{matrix}\text{sodium reference}\\ \text{electrode}\end{matrix}$$

The DTAB and sodium ions carry the same charges; hence, measurements using the above cell give the ratio (DTAB ion activity)/(sodium ion activity). Under favorable conditions the activity coefficients of the DTAB monomer cation and sodium ions are approximately equal, which in turn means that the ratio (DTAB monomer concentration)/(sodium ion concentration) is measured. Therefore, this electrode was used to determine the concentration of monomer DTAB surfactant and counter ions, respectively, by measuring their emf relative to a commercial sodium reference electrode.

Scattering Light Intensity Measurements. The time-average intensity of scattered light at 450 nm was measured. The scattered light intensity was monitored using the right-angle geometry in the synchromaters scanning region of the excitation and emission monochromators at 450 nm. In these experiments, the band width for the excitation and emission wavelengths was 3 nm. Because the measuring scattered light of a protein solution, $I_{\text{protein solution}}$, was corrected with respect to the scattered light intensity of the solvent, I_{solvent}, so that the excess intensity, I_s, was calculated from this equation, $I_s = I_{\text{protein solution}} - I_{\text{solvent}}$ (solvent contains all of the components except protein). For each protein concentration, the I_s values were determined at various DTAB concentrations. The scattered light for each solution was measured in a time interval of about 5 min, and the time-average intensity was calculated from these data. The α-amylase and DTAB solutions do not show any absorption at 450 nm and the dimensions of the scattering solute molecules are small compared with the wavelength of the incident light (450 nm).

The temperature was maintained constant at 25 °C using a thermostat cell compartment.

Results and Discussion

At DTAB concentrations below the critical micelle concentration (CMC), the DTAB was completely dissociated. Therefore, the logarithm of the concentration of DTAB against the emf gives the Nernstian slope (57–60 mV). However, at higher concentration, the resulting plots show a distinct break at the critical micelle concentration, CMC (Fig. 1).

Figure 2 shows the emf as a function of $\log[\mathrm{DTAB}]_t$ in the presence of α-amylase, at 10^{-4} M NaBr and 25 °C. Similar curves were obtained under other experimental conditions. This curve consists of three distinct regions, as follows:

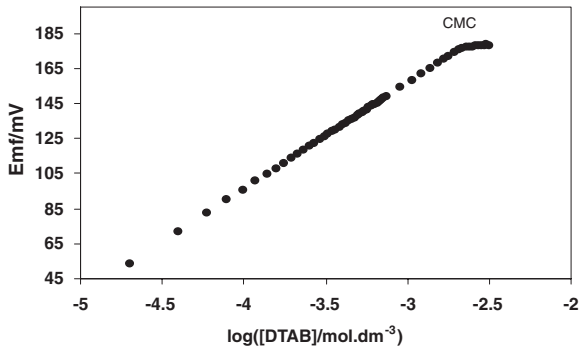

Fig. 1. The variation of emf vs $\log[\mathrm{DTAB}]_f$, at 25 °C and 10^{-4} M NaBr. The break is observed at CMC. The slope of the line before CMC is about 58 mV with high correlation coefficient which represents the Nernstian behavior. The similar plots have been obtained at other experimental conditions.

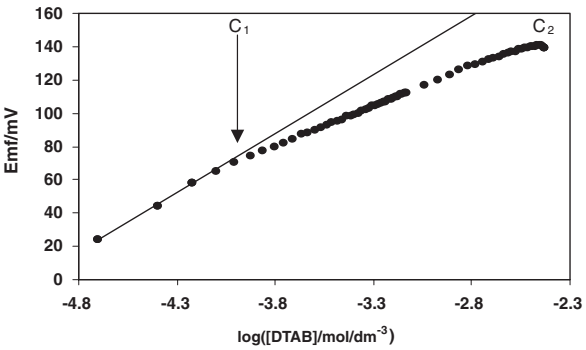

Fig. 2. The variation of emf vs $\log[\mathrm{DTAB}]_f$, at 25 °C and 10^{-4} M NaBr, in the presence of 1 mg/mL enzyme. The two successive breaks are shown by C_1 and C_2. The similar plots have been obtained at other experimental conditions.

I. The first region, which is at very low concentrations of DTAB, shows a Nernstian slope, which is approximately equal to the corresponding value in the absence of α-amylase. Hence, it can be concluded that there is no measurable interaction between α-amylase and DTAB in this region. The slope and corresponding correlation coefficient of this region under the various experimental studied conditions are listed in Table 1. These values represent the Nernestian behavior at this region.

II. The second region begins with a distinct break, which is shown as C_1 in the plot. This deviation from linearity is due to the interaction of DTAB with α-amylase, and continues until the second distinct break, shown as C_2, is reached.

III. The third region is located after C_2, where the monomer concentration gradually decreases as the total concentration of DTAB is increased. In this region, the aggregation of DTAB ions and a micelle formation occurs.

By considering the fact that the emf is reduced in the presence of α-amylase, the amount of DTAB bond to α-amylase can be calculated. The average number of DTAB molecules bound per α-amylase molecule (ν) has been calculated as

Table 1. The Value of Slope and Square of Correlation Coefficient (R^2) of the Linear Trend Line Passed through First Region in the Plot of emf vs log[DTAB]$_t$, at Various Experimental Conditions

[α-Amylase] (mg/mL)	pH	[NaBr] /M	[Urea] /M	slope	R^2
1.0	6.50	0.0001	0.0	57.8	1
2.0	6.50	0.0001	0.0	59.3	0.9965
3.0	6.50	0.0001	0.0	57.3	0.9869
1.0	6.50	0.0001	0.0	57.9	0.9990
1.0	6.50	0.0010	0.0	57.0	0.9999
1.0	6.50	0.0100	0.0	57.0	0.9999
1.0	6.50	0.1000	0.0	57.6	0.9688
1.0	9.70	0.0001	0.0	57.1	0.9990
1.0	6.50	0.0001	1.0	59.5	0.9900
1.0	6.50	0.0001	3.0	59.5	0.9900
1.0	6.50	0.0001	5.0	57.2	0.9688
1.0	6.50	0.0001	7.0	58.3	0.9930
1.0	6.50	0.0001	9.0	57.0	0.9950

$$\nu = \frac{[\mathrm{DTAB}]_t - [\mathrm{DTAB}]_f}{[\alpha\text{-amylase}]_t}, \quad (1)$$

where $[\mathrm{DTAB}]_t$, $[\mathrm{DTAB}]_f$, and $[\alpha\text{-amylase}]_t$ are the total and free concentration of DTAB and the total concentration of α-amylase, respectively.

Figure 3 shows the binding isotherm at 10^{-4} M NaBr, for the interaction of DTAB with α-amylase at various concentrations of the protein. The curves corresponding to 0.5 and 1 mg/mL of protein are approximately coincidence to each other within the experimental errors. However, at higher concentrations of α-amylase, the curves show significant differences. This behavior can be related to the aggregation state of the protein. It is well known that this enzyme has a tendency to form aggregates, and at 50 mM of K_2HPO_4, its monomer and dimmer forms are in equilibrium with each other. The aggregation phenomena can be generally shown by the following equilibrium:

$$\begin{aligned} P + P &\rightleftharpoons P_2, \\ P_2 + P &\rightleftharpoons P_3, \\ &\vdots \quad\quad \vdots \\ P_{i-1} + P &\rightleftharpoons P_i, \\ &\vdots \quad\quad \vdots \\ P_{n-1} + P &\rightleftharpoons P_n. \end{aligned} \quad (2)$$

The actual ν should be equal to the summation of the average number of bound ligands to any aggregated species (ν_i), or

$$\nu = \nu_P + \nu_{P_2} + \nu_{P_3} + \ldots + \nu_{P_i} + \ldots + \nu_{P_n}. \quad (3)$$

The precise value of each component in the above statement should be known in order to calculate the actual ν. Because this is impossible for this system, the reported ν has been calculated based on this assumption that all of the protein molecules are in the monomeric form. The coincidence of isotherms at 0.5 and 1 mg/mL of proteins represents the correctness of the monomer assumption at this concentration range. However, at higher concentrations of α-amylase, aggregation phenomena have occurred and the corresponding isotherms diverge.

For a confirmation of this idea, the corrected scattered light intensity of the protein solution at various concentrations of DTAB was determined. The results are plotted in Fig. 4. From this figure, the corrected scatter light intensity of the protein solution at 450 nm (SLI) does not show a significant change at various DTAB concentrations, which can show that the binding of DTAB does not change the aggregation state of

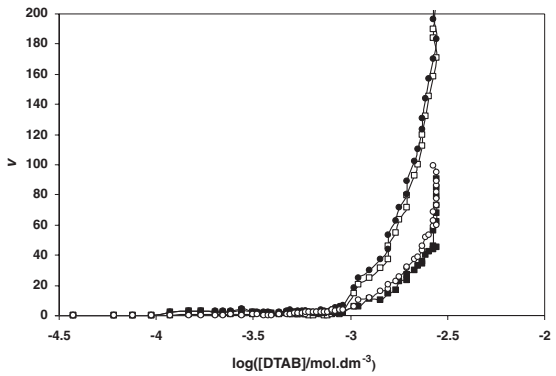

Fig. 3. Binding isotherms for interaction of DTAB with α-amylase at 25 °C, pH = 6.5, 10^{-4} M NaBr, and various protein concentrations. (□) 0.5 mg/mL, (●) 1 mg/mL, (■) 2 mg/mL, (○) 3 mg/mL.

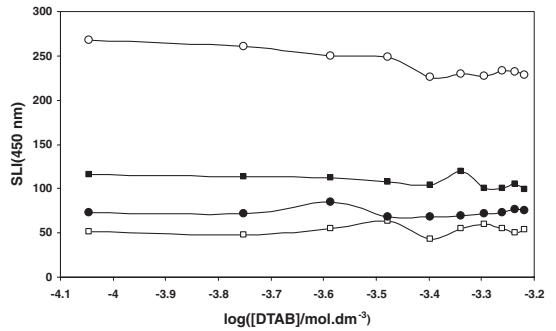

Fig. 4. The variation of corrected scatter light intensity of α-amylase solution (SLI (450 nm)) versus log[DTAB]. Various curves correspond to various protein concentrations, (□) 0.5 mg/mL, (●) 1 mg/mL, (■) 2 mg/mL, (○) 3 mg/mL, of α-amylase.

α-amylase. However, the curves corresponding to 0.5 and 1 mg/mL of protein are very closed to each other, and show significant differences with higher protein concentrations. Hence, it can be concluded that aggregation state of protein increased at concentrations higher than 1 mg/mL. This is in good agreement with potentiometric results.

From the results of this part, the value of 1 mg/mL has been selected for the protein concentration in other measurements.

Figures 5, 6, and 7 are the binding isotherms for binding of DTAB to α-amylase (1 mg/mL), at various ionic strengths, pH values, and urea concentration, respectively.

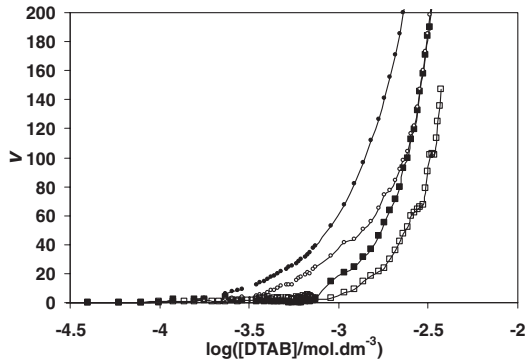

Fig. 5. Binding isotherms for interaction of DTAB with α-amylase at 25 °C, pH = 6.5, and various ionic strength. (●) 10^{-1}, (○) 10^{-2}, (□) 10^{-3}, and (■) 10^{-4} M NaBr.

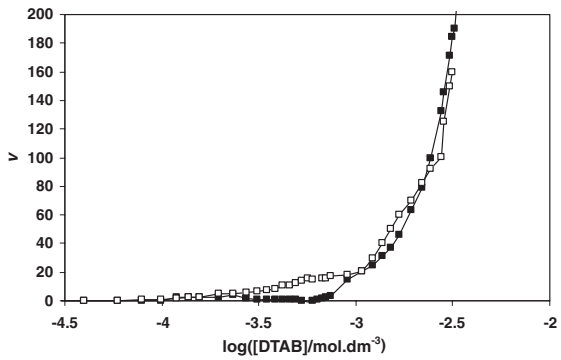

Fig. 6. Binding isotherms for interaction of DTAB with α-amylase at 25 °C, 10^{-4} M NaBr, and various pH. (■) pH = 6.5, (□) pH = 9.7.

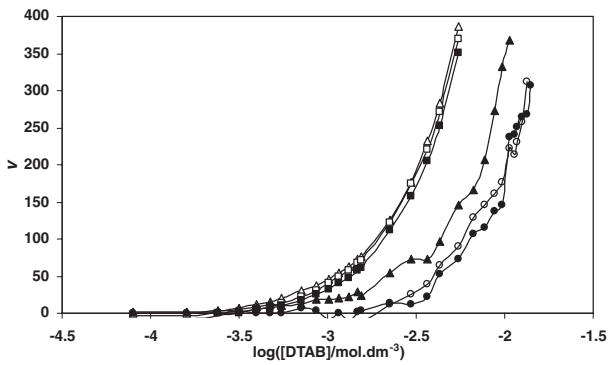

Fig. 7. Binding isotherms for interaction of DTAB with α-amylase at 25 °C and various urea concentrations, (▲) 0 M, (●) 1 M, (○) 3 M, (■) 5 M, (□) 7 M, (△) 9 M.

A calculation of the apparent binding constant ($K_{app}(\nu)$) can be applied to the entire collection of binding isotherms. This is based on the Wyman binding potential model.[17,18] The binding potential (Π) is calculated from the area under the binding isotherms according to

$$\Pi = 2.303RT \int_{[s]_i=0}^{[s]_f} \nu \, d\log[s]_f, \tag{4}$$

and is related to the apparent binding constant ($K_{app}(\nu)$) as follows:

$$\Pi = RT \ln(1 + K_{app}(\nu)[s]_f{}^{\nu}). \tag{5}$$

The values of $K_{app}(\nu)$ as a function of ν were determined by applying Eqs. 4 and 5 to determine the values of ΔG_ν,

$$\Delta G_\nu = \frac{\Delta G(\nu)}{\nu} = \frac{-RT \ln K_{app}(\nu)}{\nu}. \tag{6}$$

The plots of ΔG_ν vs $\log[\mathrm{DTAB}]_f$, which correspond to Figs. 5, 6, and 7, are shown in Figs. 8, 9, and 10, respectively.

Figure 8 shows the effect of the ionic strength in the binding affinity of DTAB to α-amylase. The binding affinity at 10^{-3} M NaBr is more than that at other NaBr concentrations. This behavior can be interpreted based on opposite effects of the ionic strength on the electrostatic and hydrophobic forces. The increasing ionic strength decreases the electrostatic interactions, and inversely increases the hydrophobic interactions. It is well known that the combinations of electrostatic and hydrophobic

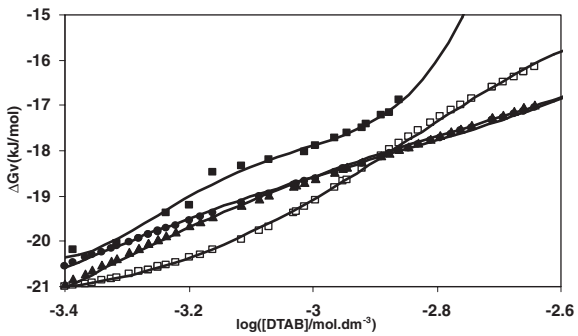

Fig. 8. Gibbs free energy of binding for interaction of DTAB with α-amylase as a function of $\log[\mathrm{DTAB}]_f$ at 25 °C and various ionic strength. (●) 10^{-1}, (▲) 10^{-2}, (□) 10^{-3}, and (■) 10^{-4} M NaBr.

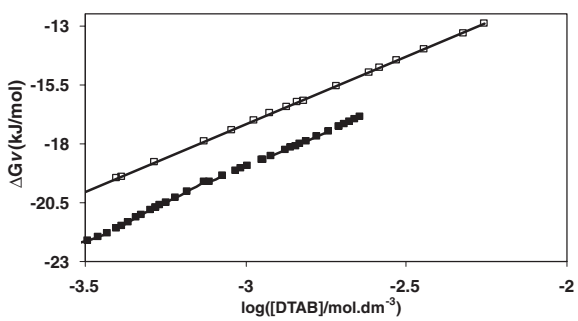

Fig. 9. Gibbs free energy of binding for interaction of DTAB with α-amylase as a function of $\log[\mathrm{DTAB}]_f$ at 25 °C and various pH. (■) pH = 6.5, (□) pH = 9.7.

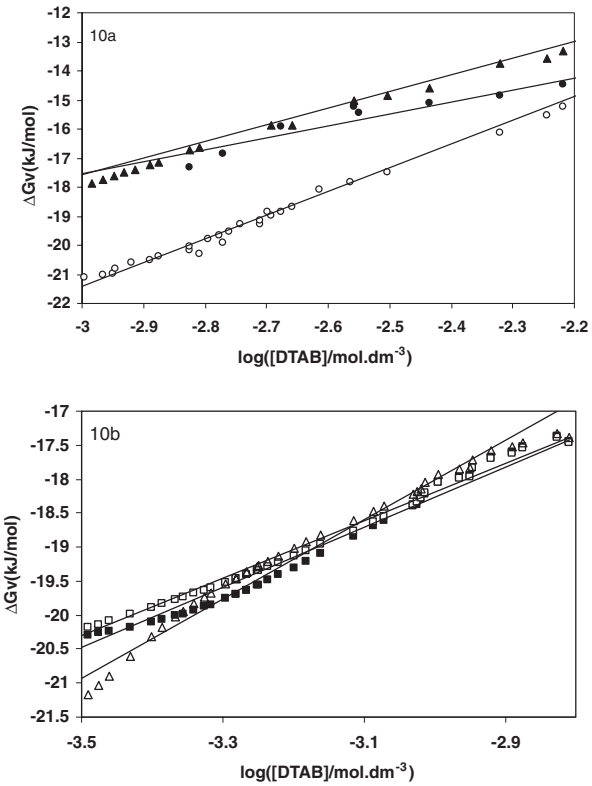

Fig. 10. Gibbs free energy of binding for interaction of DTAB with α-amylase as a function of log[DTAB] at 25 °C, pH = 6.5, 10^{-4} M NaBr, and various urea concentrations. a) (▲) 0 M, (●) 1 M, (○) 3 M, b) (■) 5 M, (□) 7 M, (△) 9 M of urea.

forces are involved in the binding of ionic surfactants to globular proteins. Hence, it can be concluded that at 10^{-3} M NaBr the net electrostatic and hydrophobic interactions is maximum.

Figure 9 represents the higher affinity of DTAB to α-amylase at pH = 6.5. The isoelectric pH of α-amylase is 3.9.[19] Therefore, all of the acidic residues are deprotonated at pH 6.5 and 9.7, and there is not any considerable difference between the net negative charge density of protein at these pH values. The previous studies showed a slight difference between the Zeta-potential and the protein stability in this pH range.[19] However, the increasing protein affinity for self aggregation occurred by increasing the pH. This mater makes the binding affinity at pH = 6.5 to become more than pH = 9.7.

Figure 10 shows the variation of ΔG_v vs log[DTAB] for interactions of DTAB with α-amylase at various urea concentrations. With respect to this figure, the maximum binding affinity of DTAB to α-amylase was observed at 3 M of urea. This behavior can be interpreted based on two opposite effects of urea in the environment and the protein structure. The presence of urea molecules breaks the ordered structure of water, and consequently decreases its hydrophobicity. This mater causes decreases in the hydrophobic interactions between the hydrocarbon tail of DTAB and hydrophobic patched at the protein surface. However, the presence of urea decreases the protein stability, and ultimately unfolds the native protein structure. The unfolding of protein exposes the hydrophobic regions of protein buried in the interior of protein in a native structure. This effect oppositely increases the interaction between protein and DTAB. The competition between these two opposite effects caused the maximum affinity to be observed at 3 M of urea. However, between 3 to 5 M of urea the binding affinity increased due to unfolding. With respect to a smaller difference in the binding affinity at urea concentrations more than 5 M, it can be concluded that the maximum unfolding of α-amylase occurred in the urea concentration range from 3 to 5 M.

Conclusion

The results represent the self aggregation of α-amylase in the presence of DTAB at concentrations of protein higher than 1 mg/mL. The tendency of α-amylase for self aggregation at a higher pH also causes a decrease of its interaction affinity with DTAB. The less affinity of DTAB to aggregate forms of α-amylase may be related to the burdening of hydrophobic patches at the protein surface during its self aggregation. The binding data analysis at various urea concentrations represents the occurrence of an unfolding process in the 3 to 5 M urea concentration range.

The financial support of Center for Graduate Studies and Research Council of Isfahan University is gratefully acknowledged.

References

1 R. Gupta, P. Gigras, H. Mohapatra, V. K. Goswami, and B. Chauhan, *Proc. Biochem.*, **38**, 1599 (2003).

2 W. W. Windish and N. S. Mhatre, "Microbial Amylases," in "Advances in Applied Microbiology," ed by W. U. Wayna, New York, Academic Press (1965), Vol. 7, p. 273.

3 A. Pandey, P. Nigam, C. R. Soccol, V. T. Soccol, D. Singh, and R. Mohan, *Biotechnol. Appl. Biochem.*, **31**, 135 (2000).

4 M. T. Jensen, T. E. Gottschalk, and B. Svensson, *J. Cereal Sci.*, **38**, 289 (2003).

5 M. Nirmala and G. Muralikrishna, *Carbohydr. Polym.*, **54**, 43 (2003).

6 J. P. Machaiah and U. K. Vakil, *J. Biosci.*, **6**, 47 (1984).

7 T. Akazawa, T. Mitsui, and M. Hayashi, *Biochem. Plants*, **14**, 465 (1988).

8 P. Talamond, V. Desseaux, Y. Moreau, M. Santimone, and G. Marchis-Mouren, *Comp. Biochem. Physiol., Part B*, **133**, 351 (2002).

9 R. Sabate and J. Estelrich, *Int. J. Biol. Macromol.*, **28**, 151 (2001).

10 E. D. Goddard, "Protein—Surfactant Interactions," ed by K. P. Ananthapadmanabhan, CRC Press, Boca Raton, New York (1993), Chap. 8.

11 A. K. Bordbar, A. A. Moosavi-Movahedi, and M. K. Amini, *Thermochim. Acta*, **400**, 95 (2003).

12 A. A. Saboury, A. K. Bordbar, and A. A. Moosavi-Movahedi, *Bull. Chem. Soc. Jpn.*, **69**, 3031 (1996).

13 A. K. Bordbar, A. A. Saboury, M. R. Hosaindokht, and A. A. Moosavi-Movahedi, *J. Colloid Interface Sci.*, **192**, 415 (1997).

14 K. H. Park, T. J. Kim, and T. J. Cheong, *Biochim. Biophys. Acta*, **1478**, 165 (2000).

15 M. A. Thomason, H. Mwakibete, and E. Wyn-Jones, *J. Chem. Soc., Faraday Trans. 1*, **86**, 1511 (1990).

16 N. Takisawa, D. G. Hall, E. Wyn-Jones, and P. Brown, *J. Chem. Soc., Faraday Trans. 1*, **84**, 3059 (1988).

17 A. K. Bordbar and A. A. Moosavi-Movahedi, *Bull. Chem. Soc. Jpn.*, **69**, 2231 (1996).
18 J. Wyman, *J. Mol. Biol.*, **11**, 631 (1965).
19 B. O. Malmstrom, *Q. Rev. Biophys.*, **6**, 389 (1974).